

# Quantum Switching of Entangled Photons based on Rydberg Blockade Effect

Dong-Sheng Ding,<sup>1, 2,\*</sup> Yi-Chen Yu,<sup>1, 2</sup> Ming-Xin Dong,<sup>1, 2</sup> Ying-Hao Ye,<sup>1, 2</sup> Guang-Can Guo,<sup>1, 2</sup> and Bao-Sen Shi<sup>1, 2, †</sup>

<sup>1</sup>*Key Laboratory of Quantum Information, University of Science and Technology of China, Hefei, Anhui 230026, China.*

<sup>2</sup>*Synergetic Innovation Center of Quantum Information and Quantum Physics, University of Science and Technology of China, Hefei, Anhui 230026, China.*

(Dated: May 2, 2022)

**The long-range Rydberg interaction endows a medium with large optical non-linearity, thus resulting in strong photon-photon interaction that are essential quantum circuits and networks. Our efforts aim at the ultimate mission of single quantum particles controlling an entire entangled system, which is a benchmark and long-term goal in quantum information science. In particular, we demonstrated coherent optical switching of entangled photons in the system of cold atomic gases under a Rydberg electromagnetically induced transparency configuration. With the presence of Rydberg blockade effect, the gate field makes the atoms non-transparent thereby blocking the single photon emitted from another atomic ensemble. In contrast to the trivial case without the gate field, the gate field excites  $N=1\sim 2$  atoms per average blockade sphere, and hence more than 50% of the entangled photons are blocked, thereby achieving effective entanglement switching. This switching of the photonic entanglement depends on the principal quantum number and the photon number of the gate field. Our experimental progress hints at quantum information processing through the interaction between Rydberg atoms and entangled photon pairs.**

In analogy to classical electronic counterparts, quantum switches are regarded as basic building blocks for quantum circuits and networks [1–3]. Switching states in the full-quantum regime where single particles control a quantum qubit or entanglement from another system may enable further applications in quantum information fields, such as in quantum computing [4], distributed quantum information processing [5] and metrology [6]. Many efforts have gone towards constructing a prototype; examples include a coupled micro-resonator with a single atom [7], trapped cold atoms in a microscopic hollow fibre [8], coupled cold atoms in a cavity operating in the strong coupling regime [9], strongly coupled quantum dots–cavity [10], and single dye molecules [11].

However, all the related experiments on switching were demonstrated with weak coherent field, thus there are no reports on switching of entangled photons. The strong interaction offered by highly excited Rydberg atoms shifts the surrounding atoms dramatically and suppresses all further excitation in the neighbour. This interaction be-

tween cold atoms gives rise to the excitation blockade [12–18], many-body entanglement [19–22], spatial correlations [23–25], strong optical non-linearities [26–32], plasma formation [33], photon-photon gate [34]. Recent works on building a single-photon transistor [35–37] exhibit the strong interaction between Rydberg atoms could be extended to single photon manipulation. Scaling a Rydberg-mediated switch device for quantum entanglement could enable the implementation of quantum computation and information processing with the interaction between Rydberg atoms and entangled photons [4], such as building a Toffoli gate [38] and quantum computation [39–42] with Rydberg ensembles, and switching a distributed quantum node.

Here, we demonstrate an experiment of quantum switching entangled photonic pairs within two atomic ensembles. The entangled photons are prepared in a two-dimensional atomic cloud and inputted into another three-dimensional atomic ensemble for switching. Because the nonlinearity offered by the Rydberg long-range interaction is larger, the Rydberg electromagnetically induced transparency (Rydberg-EIT) medium [26, 43] becomes opaque and single photons are absorbed and finally blocked. The measured coincidence counts with and without a gate field show an obvious switching of the entangled state. The fidelity of the entangled state is  $85.3\% \pm 1.5\%$  and  $80.4\% \pm 2.3\%$  in the absence and presence of a gate field, respectively, with a switch contrast larger than 50% thus beating the cloning limit [44], showing an effective switching operation. By increasing the principal quantum number  $n$ , switching become strong and the required photon number of the gate field decreases.

The sample media are optically thick atomic ensembles of Rubidium 85 ( $^{85}\text{Rb}$ ) trapped in two-dimensional (2-D) and three-dimensional (3-D) MOTs, labelled MOT 1 and MOT 2. Schematics of the energy levels, time sequence, and experimental setup are shown in figure 1(a)–(c). A 2-D  $^{85}\text{Rb}$  atomic ensemble is first prepared in MOT 1 and then cooled down to about  $100 \mu\text{K}$  via the optical molasses technique; the atomic cloud has dimensions of  $10 \times 2 \times 2 \text{ mm}^3$ . In this atomic ensemble, we prepare photon pairs by spontaneous four-wave mixing (SFWM). The energy levels involved here correspond to the double- $\Lambda$  system. The two pump fields couple the atomic transition  $5S_{1/2}(F=3) \rightarrow 5P_{1/2}(F'=3)$  with a detuning of  $-110 \times 2\pi \text{ MHz}$  and the atomic transi-

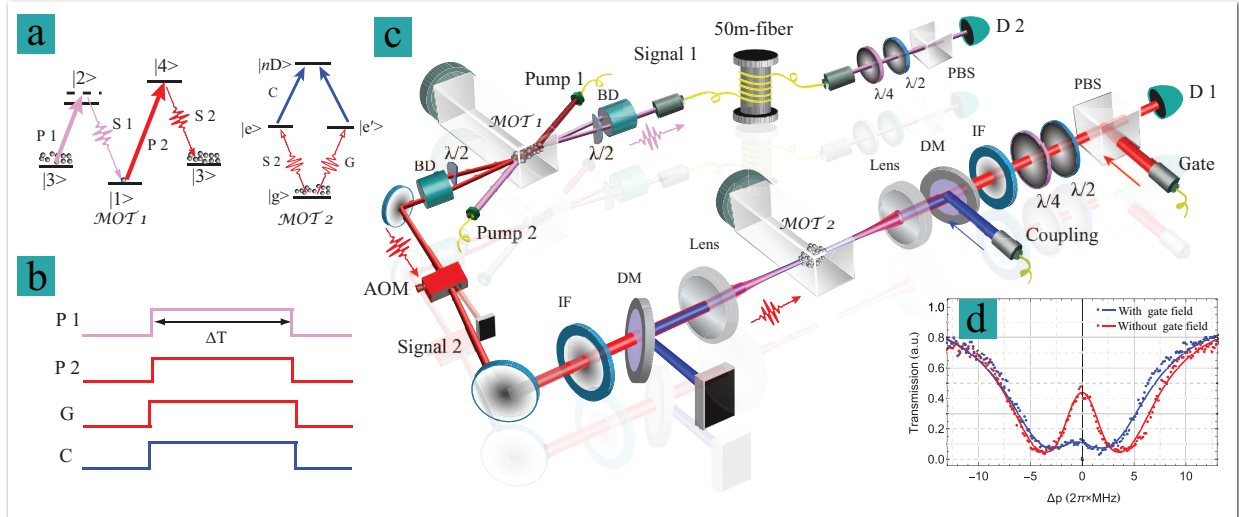


Figure 1. (a) Energy diagram of entanglement generation and photonic switch processes, including the double- $\Lambda$  atomic configuration corresponding to the  $^{85}\text{Rb}$  states of  $5S_{1/2}(F=2)$  ( $|1\rangle$ ),  $5P_{3/2}(F'=3)$  ( $|2\rangle$ ),  $5S_{1/2}(F=3)$  ( $|3\rangle$ ), and  $5P_{1/2}(F'=3)$  ( $|4\rangle$ ), respectively, and the pump fields of P1 and P2 and their respective signal fields S1 and S2; the other energy diagram is of the ladder-type Rydberg-EIT with ground state  $5S_{1/2}(F=3)$  ( $|g\rangle$ ), excited state  $5P_{3/2}(F'=4)$  ( $|e\rangle$ ), and highly-excited state  $|nD_{5/2}\rangle$  ( $|nD\rangle$ ). Labels: P-pump, S-signal. (b) Time sequence for the preparation and switching of entanglement.  $\Delta T$  represents the experimental window. (c) Schematic overview of the experimental setup, comprising two magneto-optic traps (MOT) systems, in which MOT 1 and MOT 2 are used to generate and switch the photonic entanglement, respectively. Labels: PBS-polarizing beam splitter, DM-dichroic mirror,  $\lambda/2$ -half-wave plate, IF-interference filter, D-single photon detector, BD-beam displacer, AOM-acousto-optic modulator. (d) Rydberg-EIT transmission spectra recorded with and without the gate field; both the input signal and the gate fields are weak coherent fields; the principal quantum number is  $n=50$ . The solid lines are fitted using equation 1 in Methods.

tion  $5S_{1/2}(F=2) \rightarrow 5P_{3/2}(F'=3)$  under resonance. The generated signal photons (labelled signal 1 and signal 2) are correlated in the time domain. The signal-2 photon on passing through an acousto-optic modulator (AOM) is frequency shifted  $+120 \times 2\pi$  MHz, after which the signal-2 photon is exactly resonant with the atomic transition  $5S_{1/2}(F=3) \rightarrow 5P_{3/2}(F'=4)$ . Then, the signal-2 photon is inputted into the 3-D  $^{85}\text{Rb}$  atomic cloud in the demonstration of photonic switching. This 3-D cloud has a size of  $500 \mu\text{m}$  with a temperature  $\sim 20 \mu\text{K}$  and an average density of  $3.5 \times 10^{11} \text{ cm}^{-3}$ . The signal-2 field has a beam waist of  $16 \mu\text{m}$  in the centre of MOT 2 by using a short-focus lens. With a coupling laser beam, we demonstrate Rydberg EIT in the ladder-type atomic configuration, consisting of a ground state  $|g\rangle$ , an excited state  $|e\rangle$ , and a highly-excited state  $|nD\rangle$ ; here,  $n=50$ . The van der Waals interactions between the Rydberg atoms with a  $C_6 = 2\pi \times 35 \text{ GH} \cdot \mu\text{m}^6$  for the rubidium  $50D_{5/2}(m_j=5/2)$  state, giving a blockade radius  $\sim 4.4 \mu\text{m}$  with  $r_b = |\frac{C_6}{\delta\omega}|^{1/6}$  ( $\delta\omega \sim 5 \times 2\pi$  MHz is the bandwidth of signal-2 photon) in accordance with the algorithm in Ref. [45]. The average atoms number within a blockade sphere for  $n=50$  is estimated  $\sim 350 \pm 40$ .

We first recorded the EIT spectra for a coherent field [marked in red in figure 1(d)]. For demonstrating photonic switching, we need a second coherent pulse acting

as a gate field; this field is resonant with the atomic transition  $5S_{1/2}(F=3) \rightarrow 5P_{3/2}(F'=4)$ . If we add the gate field, the medium become non-transparent because of the remarkable optical nonlinearity of the excited Rydberg

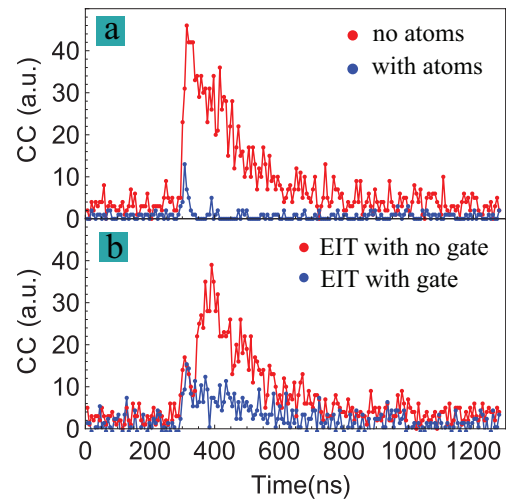


Figure 2. Measured coincidence counts (CC) under different situations corresponding to: (a) with (blue) and without atoms (red), and (b) under the Rydberg-EIT configuration with (blue) and without (red) gate field. Both these CC were recorded over an interval of 4000 s.

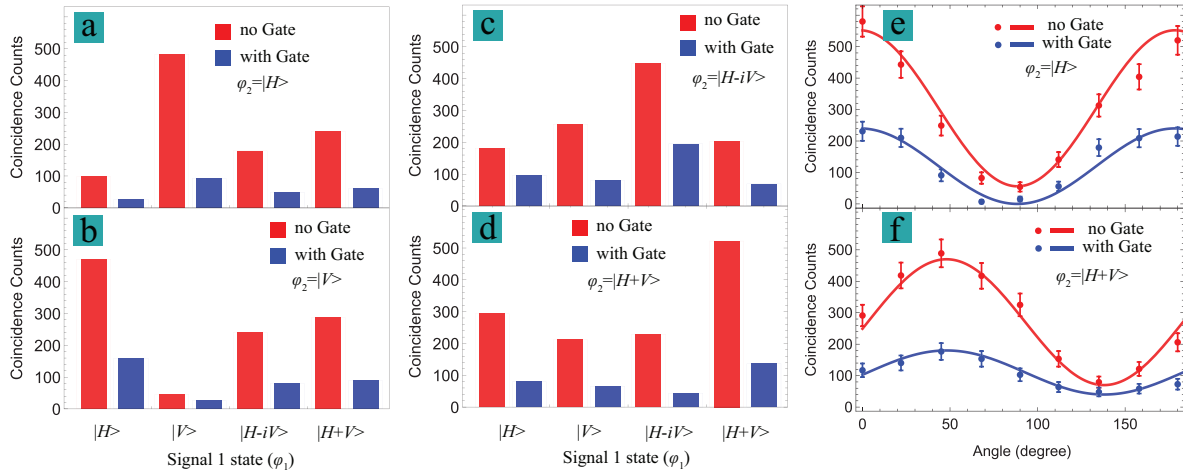


Figure 3. Switching with different bases: (a)–(d) are the coincidence counts without gate field (red bar) and with gate field (blue bar) under different signal-1 states of  $|\text{H}\rangle$ ,  $|\text{V}\rangle$ ,  $|\text{H}\rangle - i|\text{V}\rangle$ , and  $|\text{H}\rangle + |\text{V}\rangle$ . (e) and (f) are the recorded two-photon interference patterns with signal-2 states of  $|\text{H}\rangle$  and  $|\text{H}\rangle + |\text{V}\rangle$  without gate field (red) and with gate field (blue). Their interference visibilities are  $87.0\% \pm 0.8\%$  ((e), red),  $82.9\% \pm 0.7\%$  ((e), blue),  $72.0\% \pm 1.1\%$  ((f), red), and  $57.1\% \pm 2.6\%$  ((f), blue). The solid lines are fitted curves to the measured data. Both these coincidence counts were recorded over a 1000-s interval. Error bars are  $\pm 1$  standard deviation.

atoms [31] [marked in blue in figure 1(d)].

To demonstrate the Rydberg-EIT for single photons, a connection is required between the two physical systems under the quantum regime, including a matching procedure of frequency and bandwidth between the signal-2 photon and the absorption window of the atomic ensemble in MOT 2. This can be realized by changing the frequency and Rabi frequency  $\Omega_{p2}$  of the field of pump 2, see Methods for more details. For the optimized case  $\Omega_{p2} \sim 1 \times 2\pi$  MHz, the bandwidth of the signal-2 photon is at  $\sim 5 \times 2\pi$  MHz, and the absorption window for the atomic ensemble in MOT 2 is  $\sim 13 \times 2\pi$  MHz. Thus, the signal-2 photon falls completely within the Rydberg EIT window.

The central phenomenon behind the operation of a single-photon switch at the Rydberg platform is the strong nonlinearity. The long-range Rydberg interaction endows the medium with a large optical nonlinearity. The resulting dipole blockade effect makes the medium non-transparent in the Rydberg-EIT configuration [26]. We use this nonlinearity to demonstrate switching. Before demonstrating the switching of the entangled photons, we show switching for a single photon. The single photon used here is from signal 2 and is switched by applying a gate field. The results are shown in figure 2(a) and (b); the former shows the coincidence counts of photon pairs when the atoms in MOT 2 are absent (red) and present (blue), whereas the latter shows the results under Rydberg-EIT without (red) and with (blue) gate field. Obviously, coincidence counts decrease when the gate field is applied as the signal-2 photon is absorbed significantly compared with the no-gate situation. We

define a switch contrast to characterize switching,

$$C_{\text{switch}} = \frac{CC_{\text{EIT}} - CC_{\text{gate}}}{CC_{\text{EIT}}}, \quad (1)$$

where  $CC_{\text{EIT}}$  and  $CC_{\text{gate}}$  represent the coincidence counts between the signal-1 and signal-2 photons without and with gate field. From the data [figure 2(a) and (b)], we obtain a switch contrast of  $C_{\text{switch}} = 77.6\% \pm 3.1\%$ . The little peak in the rising edge comes from the high-frequency components of the single photons, which fall out the absorption window of the atoms, [marked in blue color in figure 2(a)]. In our experiment, the absorption window of atoms in MOT 2 is about  $\sim 2\pi \times 13$  MHz. Although the wave-packet of the signal-2 photon may be turned by decreasing the field power of pump 2 [46], there is always a high-frequency component in the wave-packet of the signal-2 photon, resulting in an optical precursor of single photons [47].

In our experiment, the switch effect is obviously decreased against with the bandwidth of signal 2 photon, which is given in figure 5(d). Due to the narrow transparency window in the spectrum of Rydberg-EIT, the optical response on two-photon resonance is strongly effected by the level shifts induced by Rydberg dipole-dipole interaction and the linewidths of the input lasers. This external field noise can be resolved by reducing the linewidths of the input fields [48], in which high-fidelity Rydberg atomic qubit is achieved by narrow linewidths lasers input. In the case of Rydberg-EIT, the bandwidth of signal 2 photon is optimized at  $\sim 5 \times 2\pi$  MHz, and we can observe the obvious blockade effect in Rydberg-EIT window.

To demonstrate photonic entanglement switching, we

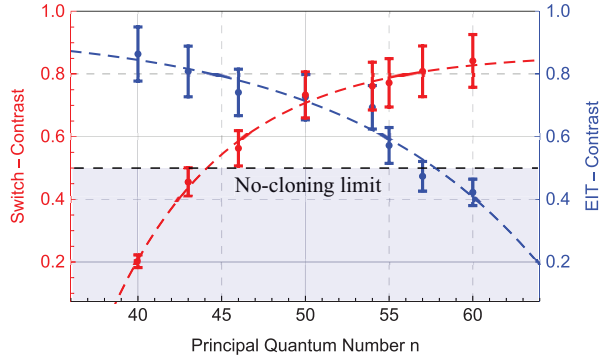


Figure 4. Dependence of the switch contrast (red) and Rydberg-EIT contrast (blue) on the principal quantum number. As visual guides, the data are fitted with function  $y = A * \text{Exp}[-x/t] + y0$  (dotted lines) with parameter settings  $A = -0.00327$ ,  $y0 = 0.94$ ,  $t = -11.77$  and  $A = -198.23$ ,  $y0 = 0.87$ ,  $t = 7.0$ . In this process, the gate field intensity is set to excite an average of  $\sim 2.1$  atoms per blockade sphere. Error bars are  $\pm 1$  standard deviation.

created passive-locking interference using techniques described in Ref. [49–52]. In this configuration, two beam displacers are used to combine the signal photons with the left and right optical paths coherently. The form of the entanglement is

$$|\psi\rangle = (|H_{s1}\rangle|V_{s2}\rangle + e^{i\varphi}|V_{s1}\rangle|H_{s2}\rangle)/\sqrt{2} \quad (2)$$

with  $\varphi$ , the relative phase between the left and right optical paths, set to zero in our experiment;  $|H_{s1,s2}\rangle$  and  $|V_{s1,s2}\rangle$  represent the horizontal and vertical polarized states of the signal photons. To demonstrate photonic entanglement switching in principle, we only block the signal-2 photons. In this situation, we use a 50-m fibre to introduce a time delay in the path of the signal-1 photons. This guarantees the entanglement does not collapse before switching has finished.

We changed the basis  $\varphi_{s2}$  of the signal-2 photon and recorded the coincidence counts under different signal-1 states  $\varphi_{s1}$  of  $|H\rangle$ ,  $|V\rangle$ ,  $|H\rangle - i|V\rangle$ , and  $|H\rangle + |V\rangle$ . To obtain the difference with and without the gate field, we recorded these coincidence counts under these situations [figure 3(a)–(d)]. The coincidence counts without (red)/with (blue) the gate field are obviously different. We obtain switch contrasts  $C_{\text{switch}}^{VH} = 81.0\%$ ,  $C_{\text{switch}}^{HV} = 64.3\%$ ,  $C_{\text{switch}}^{RR} = 52.2\%$ , and  $C_{\text{switch}}^{DD} = 79.9\%$  under the four situations  $\varphi_{s1} = |V\rangle$ ,  $\varphi_{s2} = |H\rangle$ ;  $\varphi_{s1} = |V\rangle$ ,  $\varphi_{s2} = |H\rangle$ ;  $\varphi_{s1} = \varphi_{s2} = |H\rangle - i|V\rangle$  and  $\varphi_{s1} = \varphi_{s2} = |H\rangle + |V\rangle$ . The two sets of data we obtained both exceed 50% suggesting a very promising application in which the cloning limit 50% between classical and quantum regime is required. In addition, we measured two-photon interference without and with the gate field under the signal-2 basis of  $|H\rangle$  and  $|H\rangle + |V\rangle$  [figure 3(e) and (f)]. We also have reconstructed the density matrices of the entanglement without and with the gate

field switch, and calculated the state fidelity, which are  $85.3\% \pm 1.5\%$  and  $80.4\% \pm 2.3\%$ , respectively (see Methods).

In our case, our system saturates if we further increase the photon number of the gate field. Because the gate field and the coupling field excite atoms from the ground state to Rydberg state in MOT 2 through two-photon transition, this process would deplete the atoms after a certain duration. Hence, in the experiment of switching entanglement, we set the experimental window to  $25\ \mu\text{s}$  with an average of  $\sim 1.7$  Rydberg atoms per blockade sphere. The average number of Rydberg atoms per blockade sphere is estimated by considering the atomic density, the gate field intensity and the atomic volume covered the signal 2 field.

The nonlinearity of Rydberg atoms not only depends on the Rydberg atom number, which determines the interaction distance, but also is strongly affected by the dipole interaction strength. Thus, we change the principal quantum number  $n$  to change the interaction to measure both the Rydberg-EIT transmission contrast and switch contrast. The results (figure 4) show that the Rydberg-EIT contrast decreases with increasing  $n$ ; this is because the transition amplitude for  $|e\rangle \rightarrow |nD\rangle$  decreases. In contrast, because the dipole interaction strength increases, switching of the signal-2 photon is obvious from a comparison of two situations,  $n = 60$  ( $r_b = 1.2\ \mu\text{m}$ ) and  $n = 40$  ( $r_b = 5.9\ \mu\text{m}$ ). The switch contrast is larger than 50 when  $n > 50$ , beating the quantum cloning limit [44], revealing an effective quantum blocking operation. Although the gate field has hundreds of photons because of the relatively large size of the atomic cloud in our experiment, the average  $\sim 2.1$  atoms per blockade sphere shows that switching the entanglement is realizable with a single gate-field photon when trapping atoms into the blockade radius and increasing the principal quantum number  $n$ .

In summary, we have demonstrated the optical switching of photonic entanglement based on strong photon-photon interaction within two atomic ensembles. The emitted signal-2 photon correlated with the signal-1 photon is blocked by another gate field under the Rydberg-EIT configuration. Switching effect depends on the principal quantum number, the bandwidth of the emitted single photons, and the average photon number of the gate field. We have successfully realized optical switching of entangled photons, with more than 50% of pairs being blocked. These results on switching the photonic entanglement using the strong photon-photon interaction hold promises in constructing quantum networks between Rydberg atoms and entangled photons.

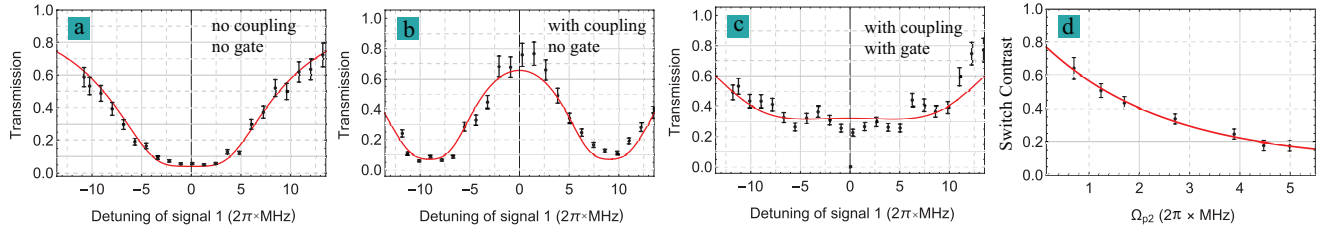


Figure 5. Transmission of the signal-2 photon under different conditions. (a) Absorption spectra of the signal-2 photon with atoms present in MOT 2. The data are fitted by function  $e^{-2Im[w_{s1}/c(1+\chi/2)]L} + a_0$  (solid lines) with parameter values of  $\Omega_c = 0$ ,  $\gamma_{eg} = 3 \times 2\pi \text{ MHz}$ ,  $\gamma_{rg} = 2 \times 2\pi \text{ MHz}$ ,  $OD = 15$ , and  $a_0 = 0.04$ . (b) Rydberg EIT effect of the signal-2 photon with coupling field present. The data are fitted by the same function above with parameter values of  $\Omega_c = 18 \times 2\pi \text{ MHz}$ ,  $\gamma_{eg} = 3 \times 2\pi \text{ MHz}$ ,  $\gamma_{rg} = 2 \times 2\pi \text{ MHz}$ ,  $OD = 15$ , and  $a_0 = 0.04$ . (c) Transmission spectra with coupling and gate fields present, the data are fitted by the same function above with parameter values of  $\Omega_c = 18 \times 2\pi \text{ MHz}$ ,  $\gamma_{eg} = 3 \times 2\pi \text{ MHz}$ ,  $\gamma_{rg} = 12 \times 2\pi \text{ MHz}$ ,  $OD = 15$ , and  $a_0 = 0.22$ . (d) The measured switch contrast against with  $\Omega_{p2}$ , the solid red curve is guided for eyes which is fitted by a function  $y = A * \text{Exp}[-x/t] + y_0$  with parameters of  $A = 0.73481$ ;  $y_0 = 0.07865$ ;  $t = 2.45$ .

## MATERIALS AND METHODS

**Experimental time sequence.** The repetition rate of our experiment is 200 Hz, and the MOT trapping time is 4.71 ms. Moreover, the experimental window is 290  $\mu\text{s}$ . The fields of pumps 1 and 2 are controlled by two AOMs, and therefore the frequencies of signals 1 and 2 photons can be tuned. The optical depth in MOT 1 is about 20. Two lenses L1 and L2, each with a focal length of 300 mm, are used to couple the signal fields into the atomic ensemble in MOT 1. The fields of pumps 1 and 2 are collinear, and hence their respective signal fields are collinear. The vector matching condition  $k_{p1} - k_{S1} = k_{p2} - k_{S2}$  is satisfied in the spontaneous four-wave mixing process, as the methods are the same as in our previous work [53]. The two signal photons are collected into their respective single-mode fibers and are detected by two single photon detectors (avalanche diode, PerkinElmer SPCM-AQR-16-FC, 60% efficiency, maximum dark count rate of 25/s). The two detectors are gated by an arbitrary function generator. The gated signals from the two detectors are then sent to a time-correlated single photon counting system (TimeHarp 260) to measure their time-correlated function.

**Frequency matching between signal 2 and atoms in MOT 2.** Connecting two different physical systems requires matching the frequency windows. For this point, the emitted signal-2 photon from MOT 1 may not be matched with the working window of Rydberg EIT in MOT 2. The detuning of the signal-2 photon is performed by changing the frequency of the pump-2 field, which is controlled by an AOM. The pump 2 field passes through the AOM, the frequency being tuned from  $-12 \sim 17 \times 2\pi \text{ MHz}$ . There is another AOM added in the optical path of the signal-2 photon (see figure 1), which afterwards has frequency  $+120 \times 2\pi \text{ MHz}$ . By this method, the frequency of the signal-2 photon can be tuned from the atomic transition  $5S_{1/2}(F = 3) \rightarrow 5P_{3/2}(F' = 3)$  to the atomic transition  $5S_{1/2}(F = 3) \rightarrow$

$5P_{3/2}(F' = 4)$ . Because the signal-2 photon falls into the atomic transition window  $5S_{1/2}(F = 3) \rightarrow 5P_{3/2}(F' = 4)$  in MOT 2, then by changing the frequency of the emitted signal-2 photon, we measure its transmission spectra (figure 5). To check this process, we added a coupling field, which is resonant with the atomic transition  $5P_{3/2}(F' = 3) \rightarrow 50D_{5/2}$ , to demonstrate the Rydberg EIT. Under the plane-wave approximation, the EIT transmission has the form  $e^{-2Im[w_{s2}/c(1+\chi/2)]L}$ , where  $L$  is the length of the atomic medium,  $w_{s2}$  the frequency of the signal 2 photon,  $c$  the speed of light in a vacuum, and  $\chi$  denotes the linear susceptibility (complex) defined as [54]

$$\chi = \frac{\alpha_0}{k_0} \frac{4(\Delta w_{s2} + i\gamma_{rg})\gamma_{eg}}{\Omega_c^2 - 4(\Delta w_{s2} + i\gamma_{rg})(\Delta w_{s2} + i\gamma_{eg})} \quad (3)$$

where  $\alpha_0 = OD/L$  is the absorption coefficient when the coupling field is not present,  $OD$  is the optical depth of atomic ensemble.  $k_0$  is the wave vector.  $\Delta w_{s2}$  is the detuning of the signal-2 photon.  $\gamma_{eg}$ ,  $\gamma_{rg}$  are the corresponding decay rates of atomic transition  $|e\rangle \rightarrow |g\rangle$  and  $|nD\rangle \rightarrow |g\rangle$ .  $\Omega_c$  represents the Rabi frequency of coupling field. We use this equation 3 to simulate the results given in figure 5(a) and (b).

The strong dipole interaction couples the nearby Rydberg atoms so that the evolution of these atoms is fundamentally linked, thereby modifying the individual atomic energy levels and lifetimes [55]. As a result of the Rydberg dipole interactions, the behaviour of an ensemble of  $N$ -atoms cannot simply be described by summing the response of a single atom  $N$  times. When we apply a weak coherent gate field, the response of the atoms cannot be described by equation 3, which refers to a single body; if there are no Rydberg dipole interactions, the transmission of the  $N$ -atom system can be traced to a summation of  $N$  single-atom contributions. To describe the behaviour for Rydberg EIT with a gate field, we use a simplifying assumption  $\gamma_{rg} \rightarrow \xi \cdot \gamma_{rg}$  where  $\xi$  is the cooperative gain coefficient. The atomic decay rate

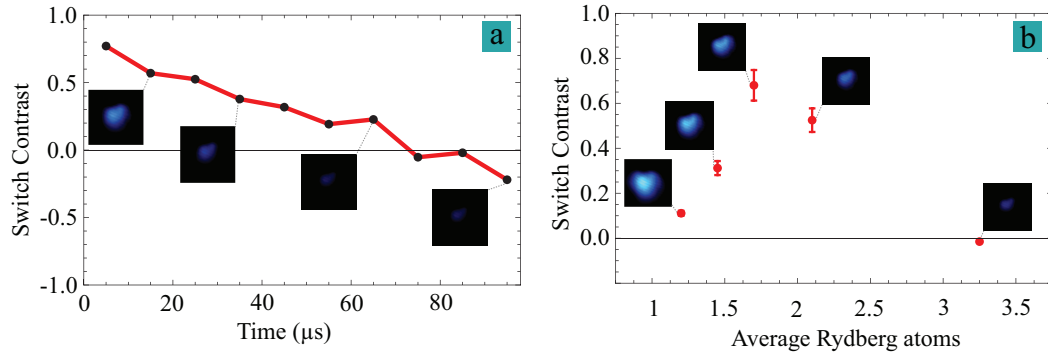


Figure 6. (a) Variation of the switch contrast with an average  $\sim 2.1$  Rydberg atoms per blockade sphere; (b) Dependence of the switch contrast on average Rydberg atoms number per blockade sphere, the time duration is set to be  $25\mu\text{s}$ . Linked to a certain data point is a fluorescence image of the atoms recorded using an electron-multiplying CCD camera.

would then increase when the Rydberg atoms interact, and the response of each atom is modified significantly. Because of this process, the response of Rydberg atoms would exhibit non-transparency behaviour for single photons when  $\xi$  is sufficiently large. Thus, we can control the single photon transmission behaviour of Rydberg EIT depending on whether nearby Rydberg atoms are excited. The Rydberg EIT effect with a gate field was measured [figure 5(c), red solid line] and the results fitted curve for  $\xi = 6$ .

**Bandwidth matching between signal 2 and atoms in MOT 2.** In this process, bandwidth mismatching between the signal-2 photon and the atomic ensemble in MOT 2 decreases the switch contrast. Because the high-frequency component of the signal-2 photon is unable to fall within the Rydberg EIT window, the reabsorption of the signal-2 photon weakens although the gate field is present; see figure 5 (d). The switch contrast decreases with increasing Rabi frequency  $\Omega_{p2}$  of pump 2 field. The bandwidth of the signal-2 photon depends significantly on  $\Omega_{p2}$  [46, 56], because the profile of the wave packet of the signal-2 photon changes through tuning the  $\Lambda$ -EIT transparent window. This result plotted in figure 5 (d) tells us that switching is better with a narrower bandwidth for the signal-2 photon. For the optimized case, the bandwidth of the signal-2 photon is measured to be  $\sim 5 \times 2\pi$  MHz, and the absorption window for the atomic ensemble in MOT 2 is  $\sim 13 \times 2\pi$  MHz. That is, the signal-2 photon can completely fall within the Rydberg EIT window.

**Threshold against excited Rydberg atoms.** Continuously exciting the atoms from ground state to Rydberg state would deplete the atoms in MOT 2 finally. Because highly-excited Rydberg atoms decay to other atomic levels via non-cycle transitions, we therefore changed the photon number of the gate field and the time duration to measure switch contrast. The results (figure 6) show switch contrast versus time duration with an average Rydberg atoms number per block-

ade sphere is  $\sim 2.1$ , and measured switch contrast versus photon number of the gate field setting the time duration at  $25\mu\text{s}$ . There is an obvious peak when the average Rydberg atoms number per blockade sphere is  $\sim 1.7$ . With increasing the photon number, the atoms are clearly depleted as evident in the weakened fluorescence image of the atoms.

#### Quantum state tomography of photonic entanglement.

We have also performed quantum state tomography [57] for the photonic entanglement to compare the entanglement properties before and after gate field switching. Signals 1 and 2 are polarization entangled, their entangled state being  $|\psi\rangle = (|H\rangle_{S1}|V\rangle_{S2} + |V\rangle_{S1}|H\rangle_{S2})/\sqrt{2}$ , here,  $|H\rangle_{S1/S2}$  and  $|V\rangle_{S1/S2}$  represent signals 1 and 2 carrying the horizontal and vertical component of the polarization. Using the polarizing beam splitter, half-wave plate, and quarter-wave plate, we projected the two photon states onto the four polarization states  $|\phi_{1\sim 4}\rangle$  ( $|H\rangle$ ,  $|V\rangle$ ,  $(|H\rangle - i|V\rangle)/\sqrt{2}$ ,  $(|H\rangle + |V\rangle)/\sqrt{2}$ ). We obtained then a set of 16 data points from which to reconstruct the density matrix. By comparing the ideal density matrix  $\rho_{ideal}$  for these four states, and using  $F = \text{Tr}(\sqrt{\sqrt{\rho}\rho_{ideal}\sqrt{\rho}})^2$ , we found the fidelity for the input and output states to be  $85.3\% \pm 1.5\%$  and  $80.4\% \pm 2.3\%$ , respectively. The fidelity is not clearly decreasing because switching is effective for any polarization state. The trend is consistent with single qubit switching demonstrated above. The error bars in our experiment are estimated by Poisson statistics using Monte Carlo simulations with the aid of Mathematica software.

**Acknowledgments** The authors thank Prof. Lin Li from huazhong university of science and technology and Prof. Yuan Sun from national university of defense technology for valued discussions and critical reading our manuscript. This work was supported by National Key R&D Program of China (2017YFA0304800), the National Natural Science Foundation of China (Grant Nos. 61525504, 61722510, 61435011, 11174271,

61275115, 11604322), and the Innovation Fund from CAS, Anhui Initiative in Quantum Information Technologies (AHY020200). **Author contributions** Dong-Sheng Ding and Yi-Chen Yu contribute to this paper equally. D.S.D. conceived the idea and experiment. D.S.D. and Y.C.Y. designed and carried out the experiments with assistance from M.X.D. and Y.H.Y.. D.S.D. wrote the manuscript with contributions from B.S.S.. D.S.D., B.S.S. and G.C.G. supervised the project. **Competing financial interests** The authors declare no competing financial interests.

\* dds@ustc.edu.cn  
† drshi@ustc.edu.cn

[1] Juan Ignacio Cirac, Peter Zoller, H Jeff Kimble, and Hideo Mabuchi, “Quantum state transfer and entanglement distribution among distant nodes in a quantum network,” *Phys. Rev. Lett.* **78**, 3221 (1997).

[2] Jeremy L O’Brien, Akira Furusawa, and Jelena Vučković, “Photonic quantum technologies,” *Nat. Photon.* **3**, 687 (2009).

[3] H John Caulfield and Shlomi Dolev, “Why future supercomputing requires optics,” *Nat. Photon.* **4**, 261 (2010).

[4] Mark Saffman, TG Walker, and Klaus Mølmer, “Quantum information with rydberg atoms,” *Reviews of Modern Physics* **82**, 2313 (2010).

[5] H Jeff Kimble, “The quantum internet,” *Nature* **453**, 1023 (2008).

[6] Peter Komar, Eric M Kessler, Michael Bishof, Liang Jiang, Anders S Sørensen, Jun Ye, and Mikhail D Lukin, “A quantum network of clocks,” *Nat. Phys.* **10**, 582 (2014).

[7] Danny O’Shea, Christian Junge, Jürgen Volz, and Arno Rauschenbeutel, “Fiber-optical switch controlled by a single atom,” *Phys. Rev. Lett.* **111**, 193601 (2013).

[8] Michal Bajcsy, Sebastian Hofferberth, Vlatko Balic, Thibault Peyronel, Mohammad Hafezi, Alexander S Zibrov, Vladan Vuletić, and Mikhail D Lukin, “Efficient all-optical switching using slow light within a hollow fiber,” *Phys. Rev. Lett.* **102**, 203902 (2009).

[9] Wenlan Chen, Kristin M Beck, Robert Bücker, Michael Gullans, Mikhail D Lukin, Haruka Tanji-Suzuki, and Vladan Vuletić, “All-optical switch and transistor gated by one stored photon,” *Science* , 1237242 (2013).

[10] Thomas Volz, Andreas Reinhard, Martin Winger, Antonio Badolato, Kevin J Hennessy, Evelyn L Hu, and Ataç Imamoglu, “Ultrafast all-optical switching by single photons,” *Nat. Photon.* **6**, 605 (2012).

[11] Jaesuk Hwang, Martin Pototschnig, Robert Lettow, Gert Zumofen, Alois Renn, Stephan Götzinger, and Vahid Sandoghdar, “A single-molecule optical transistor,” *Nature* **460**, 76 (2009).

[12] Daniel Comparat and Pierre Pillet, “Dipole blockade in a cold rydberg atomic sample [invited],” *JOSA B* **27**, A208–A232 (2010).

[13] D Jaksch, JI Cirac, P Zoller, SL Rolston, R Côté, and MD Lukin, “Fast quantum gates for neutral atoms,” *Phys. Rev. Lett.* **85**, 2208 (2000).

[14] MD Lukin, M Fleischhauer, R Cote, LM Duan, D Jaksch, JI Cirac, and P Zoller, “Dipole blockade and quantum information processing in mesoscopic atomic ensembles,” *Phys. Rev. Lett.* **87**, 037901 (2001).

[15] D Tong, SM Farooqi, J Stanojevic, S Krishnan, YP Zhang, R Côté, EE Eyler, and PL Gould, “Local blockade of rydberg excitation in an ultracold gas,” *Phys. Rev. Lett.* **93**, 063001 (2004).

[16] Kilian Singer, Markus Reetz-Lamour, Thomas Amthor, Luis Gustavo Marcassa, and Matthias Weidemüller, “Suppression of excitation and spectral broadening induced by interactions in a cold gas of rydberg atoms,” *Phys. Rev. Lett.* **93**, 163001 (2004).

[17] E Urban, Todd A Johnson, T Henage, L Isenhower, DD Yavuz, TG Walker, and M Saffman, “Observation of rydberg blockade between two atoms,” *Nature Physics* **5**, 110 (2009).

[18] Alpha Gaëtan, Yevhen Miroshnychenko, Tatjana Wilk, Amodsen Chotia, Matthieu Viteau, Daniel Comparat, Pierre Pillet, Antoine Browaeys, and Philippe Grangier, “Observation of collective excitation of two individual atoms in the rydberg blockade regime,” *Nat. Phys.* **5**, 115 (2009).

[19] Rolf Heidemann, Ulrich Raitzsch, Vera Bendkowsky, Björn Butscher, Robert Löw, Luis Santos, and Tilman Pfau, “Evidence for coherent collective rydberg excitation in the strong blockade regime,” *Phys. Rev. Lett.* **99**, 163601 (2007).

[20] Johannes Zeiher, Peter Schauß, Sebastian Hild, Tommaso Macrì, Immanuel Bloch, and Christian Gross, “Microscopic characterization of scalable coherent rydberg superatoms,” *Phys. Rev. X* **5**, 031015 (2015).

[21] Henning Labuhn, Daniel Barredo, Sylvain Ravets, Sylvain De Léséleuc, Tommaso Macrì, Thierry Lahaye, and Antoine Browaeys, “Tunable two-dimensional arrays of single rydberg atoms for realizing quantum ising models,” *Nature* **534**, 667–684 (2016).

[22] Hannes Bernien, Sylvain Schwartz, Alexander Keesling, Harry Levine, Ahmed Omran, Hannes Pichler, Soonwon Choi, Alexander S Zibrov, Manuel Endres, Markus Greiner, *et al.*, “Probing many-body dynamics on a 51-atom quantum simulator,” *Nature* **551**, 579 (2017).

[23] Peter Schauß, Marc Cheneau, Manuel Endres, Takeshi Fukuhara, Sebastian Hild, Ahmed Omran, Thomas Pohl, Christian Gross, Stefan Kuhr, and Immanuel Bloch, “Observation of spatially ordered structures in a two-dimensional rydberg gas,” *Nature* **491**, 87–91 (2012).

[24] Andrew Schwarzkopf, RE Sapiro, and Georg Raithel, “Imaging spatial correlations of rydberg excitations in cold atom clouds,” *Phys. Rev. Lett.* **107**, 103001 (2011).

[25] Peter Schauß, Johannes Zeiher, Takeshi Fukuhara, Sebastian Hild, Marc Cheneau, T Macrì, Thomas Pohl, Immanuel Bloch, and Christian Groß, “Crystallization in ising quantum magnets,” *Science* **347**, 1455–1458 (2015).

[26] Jonathan D Pritchard, D Maxwell, Alexandre Gauguet, Kevin J Weatherill, MPA Jones, and Charles S Adams, “Cooperative atom-light interaction in a blockaded rydberg ensemble,” *Phys. Rev. Lett.* **105**, 193603 (2010).

[27] YO Dudin and A Kuzmich, “Strongly interacting rydberg excitations of a cold atomic gas,” *Science* **336**, 887–889 (2012).

[28] Thibault Peyronel, Ofer Firstenberg, Qi-Yu Liang, Sebastian Hofferberth, Alexey V Gorshkov, Thomas Pohl, Mikhail D Lukin, and Vladan Vuletić, “Quantum nonlinear optics with single photons enabled by strongly in-

teracting atoms," *Nature* **488**, 57 (2012).

[29] D Maxwell, DJ Szwier, D Paredes-Barato, H Busche, JD Pritchard, Alexandre Gauguet, KJ Weatherill, MPA Jones, and CS Adams, "Storage and control of optical photons using rydberg polaritons," *Phys. Rev. Lett.* **110**, 103001 (2013).

[30] Christoph Tresp, Przemyslaw Bienias, Sebastian Weber, Hannes Gorniaczyk, Ivan Mirgorodskiy, Hans Peter Büchler, and Sebastian Hofferberth, "Dipolar dephasing of rydberg d-state polaritons," *Phys. Rev. Lett.* **115**, 083602 (2015).

[31] Ofer Firstenberg, Charles S Adams, and Sebastian Hofferberth, "Nonlinear quantum optics mediated by rydberg interactions," *Journal of Physics B: Atomic, Molecular and Optical Physics* **49**, 152003 (2016).

[32] Callum R Murray and Thomas Pohl, "Coherent photon manipulation in interacting atomic ensembles," *Phys. Rev. X* **7**, 031007 (2017).

[33] M Robert-de Saint-Vincent, CS Hofmann, H Schempp, G Günter, S Whitlock, and M Weidemüller, "Spontaneous avalanche ionization of a strongly blockaded rydberg gas," *Phys. Rev. Lett.* **110**, 045004 (2013).

[34] Daniel Tiarks, Steffen Schmidt-Eberle, Thomas Stolz, Gerhard Rempe, and Stephan Dürr, "A photon–photon quantum gate based on rydberg interactions," *Nature Physics* **15**, 124 (2019).

[35] Daniel Tiarks, Simon Baur, Katharina Schneider, Stephan Dürr, and Gerhard Rempe, "Single-photon transistor using a förster resonance," *Phys. Rev. Lett.* **113**, 053602 (2014).

[36] Hannes Gorniaczyk, Christoph Tresp, Johannes Schmidt, Helmut Fedder, and Sebastian Hofferberth, "Single-photon transistor mediated by interstate rydberg interactions," *Phys. Rev. Lett.* **113**, 053601 (2014).

[37] Simon Baur, Daniel Tiarks, Gerhard Rempe, and Stephan Dürr, "Single-photon switch based on rydberg blockade," *Phys. Rev. Lett.* **112**, 073901 (2014).

[38] David G Cory, MD Price, W Maas, E Knill, Raymond Laflamme, Wojciech H Zurek, Timothy F Havel, and SS Somaroo, "Experimental quantum error correction," *Phys. Rev. Lett.* **81**, 2152 (1998).

[39] Alexey V Gorshkov, Johannes Otterbach, Michael Fleischhauer, Thomas Pohl, and Mikhail D Lukin, "Photon–photon interactions via rydberg blockade," *Physical review letters* **107**, 133602 (2011).

[40] Mohammadsadegh Khazali, Khabat Heshami, and Christoph Simon, "Photon-photon gate via the interaction between two collective rydberg excitations," *Physical Review A* **91**, 030301 (2015).

[41] Andrew CJ Wade, Marco Mattioli, and Klaus Mølmer, "Single-atom single-photon coupling facilitated by atomic-ensemble dark-state mechanisms," *Physical Review A* **94**, 053830 (2016).

[42] Yuan Sun and Ping-Xing Chen, "Analysis of atom–photon quantum interface with intracavity rydberg-blocked atomic ensemble via two-photon transition," *Optica* **5**, 1492–1501 (2018).

[43] David Petrosyan, Johannes Otterbach, and Michael Fleischhauer, "Electromagnetically induced transparency with rydberg atoms," *Phys. Rev. Lett.* **107**, 213601 (2011).

[44] Frédéric Grosshans and Philippe Grangier, "Quantum cloning and teleportation criteria for continuous quantum variables," *Physical Review A* **64**, 010301 (2001).

[45] Nikola Šibalić, Jonathan D Pritchard, Charles S Adams, and Kevin J Weatherill, "Arc: An open-source library for calculating properties of alkali rydberg atoms," *Computer Physics Communications* **220**, 319–331 (2017).

[46] Kaiyu Liao, Hui Yan, Junyu He, Shengwang Du, Zhi-Ming Zhang, and Shi-Liang Zhu, "Subnatural-linewidth polarization-entangled photon pairs with controllable temporal length," *Phys. Rev. Lett.* **112**, 243602 (2014).

[47] Shanchao Zhang, JF Chen, Chang Liu, MMT Loy, George KL Wong, and Shengwang Du, "Optical precursor of a single photon," *Phys. Rev. Lett.* **106**, 243602 (2011).

[48] Harry Levine, Alexander Keesling, Ahmed Omran, Hannes Bernien, Sylvain Schwartz, Alexander S Zibrov, Manuel Endres, Markus Greiner, Vladan Vuletić, and Mikhail D Lukin, "High-fidelity control and entanglement of rydberg-atom qubits," *Physical review letters* **121**, 123603 (2018).

[49] Dong-Sheng Ding, Kai Wang, Wei Zhang, Shuai Shi, Ming-Xin Dong, Yi-Chen Yu, Zhi-Yuan Zhou, Bao-Sen Shi, and Guang-Can Guo, "Entanglement between low- and high-lying atomic spin waves," *Phys. Rev. A* **94**, 052326 (2016).

[50] Wei Zhang, Dong-Sheng Ding, Ming-Xin Dong, Shuai Shi, Kai Wang, Shi-Long Liu, Yan Li, Zhi-Yuan Zhou, Bao-Sen Shi, and Guang-Can Guo, "Experimental realization of entanglement in multiple degrees of freedom between two quantum memories," *Nat. Commun.* **7**, 13514 (2016).

[51] Wei Zhang, Dong-Sheng Ding, Yu-Bo Sheng, Lan Zhou, Bao-Sen Shi, and Guang-Can Guo, "Quantum secure direct communication with quantum memory," *Phys. Rev. Lett.* **118**, 220501 (2017).

[52] Yi-Chen Yu, Dong-Sheng Ding, Ming-Xin Dong, Shuai Shi, Wei Zhang, and Bao-Sen Shi, "Self-stabilized narrow-bandwidth and high-fidelity entangled photons generated from cold atoms," *Phys. Rev. A* **97**, 043809 (2018).

[53] Dong-Sheng Ding, Zhi-Yuan Zhou, Bao-Sen Shi, and Guang-Can Guo, "Single-photon-level quantum image memory based on cold atomic ensembles," *Nature communications* **4**, 2527 (2013).

[54] Shanchao Zhang, JF Chen, Chang Liu, Shuyu Zhou, MMT Loy, George Ke Lun Wong, and Shengwang Du, "A dark-line two-dimensional magneto-optical trap of 85rb atoms with high optical depth," *Review of Scientific Instruments* **83**, 073102 (2012).

[55] James Keaveney, *Collective Atom–Light Interactions in Dense Atomic Vapours* (Springer, 2014).

[56] Shengwang Du, Jianming Wen, and Morton H Rubin, "Narrowband biphoton generation near atomic resonance," *JOSA B* **25**, C98–C108 (2008).

[57] Daniel FV James, Paul G Kwiat, William J Munro, and Andrew G White, "Measurement of qubits," *Phys Rev A* **64**, 052312.